www.arpnjournals.com

REGIONAL VALIDATION OF RETRACKED SEA LEVELS FROM SARAL/ALTIKA OVER THE SOUTH CHINA SEA AND ADJACENT SEAS

Noor Nabilah Abdullah[1], Nurul Hazrina Idris[1,2], Nurul Hawani Idris[1], Muhammad Zulkarnain Abdul Rahman[1] and Wan Hazli Wan Kadir[1]

[1]Faculty of Geoinformation and Real Estate, Universiti Teknologi Malaysia, Johor Bahru, Malaysia
[2]Geoscience and Digital Earth Centre, Research Institute for Sustainability and Environment, Universiti Teknologi Malaysia, Johor Bahru, Malaysia
E-Mail: nurulhazrina@utm.my

ABSTRACT

This paper focuses on assessing the quality of sea level anomaly (SLA) data from the new generation of Ka-band SARAL/AltiKa satellite altimetry over the continental shelf of the South China Sea. The region consists of peninsulas, shallow seas, and small islands that produce complicated altimetric waveform patterns. The improved-accuracy of SLAs data from the MLE4, Ice1 and Ice2 retrackers which are provided in the AVISO-Sensor Geophysical Data Records (SGDR) were optimized in this study. The quality of retracked SLAs is assessed by making comparison with tide gauge data from six stations. In general, the percentage of data availability of Ice-1 retracker is superior (>68%) to those of MLE-4 and Ice-2 retrackers. The improvement of percentage (IMP) also shows that Ice-1 retracker improves the standard deviation >12% better than those of Ice-2 retracker. Over complex areas of Lubang and Ko Taphao Noi, the temporal correlation of Ice-1 retracker is superior ($r>0.80$) to those of MLE4 and Ice-2 retrackers ($r<0.84$). The root mean square error (RMS) error of Ice-1 retracker is the smallest (<10 cm) when compared to the other two retrackers over both regions. On the other hand, over Vung Tau, Geting and Bintulu, Ice-2 and MLE-4 retrackers have better correlations ($r>5.8$) and lower RMS error (<34 cm) than those of Ice-1 retracker. It can be concluded that the Ice-1 and Ice-2 retrackers were superior for the coastal region of Maritime Continent.

Keywords: SARAL/AltiKa, satellite altimetry, coastal sea level, tide gauge, maritime continent.

1. INTRODUCTION

A demand for accurate coastal altimetry data, especially at sea level, has arisen since human activities are intense over these regions. Near coastal areas, altimetry data become unreliable as the measured surface rapidly changes between ocean and land (Deng, *et al.,* 2002, Idris and Deng, 2012). The gap in data availability over coastal areas and continental shelf seas observed by satellite altimetry has become a main discussion among researchers for the past ten years.

In the vicinity of land, the leading edge of ocean return waveform deviates from the on-board altimeter tracking gate, which causes erroneous telemetered range measurement (Gommenginger, *et al.,* 2011). A return waveform is the received power sampled at the satellite and results from the interaction of the altimeter's transmitted pulse with the scattering surface. Altimeter waveform over homogeneous ocean surfaces (Figure-1) can be described by the Brown (1977) model. Over heterogeneous surfaces (e.g. coastal ocean and continental shelf), complex waveform shapes (Figure-1) are usually recorded since the altimeter footprint is contaminated by the multiplicity of surfaces. This contamination produces complex waveform shapes that may lead to false results in the SLA estimations.

Accurate SLA measurements over heterogeneous surfaces can be retrieved via a ground post-processing method called 'retracking' (e.g. Deng and Featherstone, 2006, Idris and Deng, 2013, Passaro, *et al.,* 2014, Tseng, *et al.,* 2014) to improve the range estimates, and by applying ocean geophysical corrections for coastal oceans (e.g. Andersen and Scharroo, 2011; Fernandes, *et al.,*

2008, Obligis, *et al.,* 2011, Obligis, *et al.,* 2008). These two components: the range and geophysical corrections (e.g. tides, wet tropospheric and sea state bias), require special treatments when attempting to retrieve sea levels over coastal areas because they are usually corrupted due to land contamination and coastal sea states.

The retracking of a waveform computes the departure of the waveform's leading edge from the tracking gate and corrects the satellite range measurement, and SLA accordingly. A wealth of innovative ideas is continuously emerging to provide alternative ways of achieving better accuracy of altimeter data from noisy waveforms near shore. These include modification of the standard Brown model (e.g. Thibaut, *et al.,* 2011) to fit the noisy coastal waveforms, retracking of multiple waveforms (e.g. Kuo, *et al.,* 2011; Quartly, 2010; Strachan and Vidale, 2013; Thibaut, *et al.,* 2009) to exploit the inter-waveform properties, and retracking of reduced gate of waveforms (e.g. AVISO, 2010; Bao, *et al.,* 2009; Idris and Deng, 2012; Lee, *et al.,* 2008) to exclude non-ocean signals. Several researches have employed multiple retracking algorithms to select the optimum retracker for retracking all waveforms via expert system (e.g. Berry, *et al.,* 1998; Deng and Featherstone, 2006; Idris and Deng, 2013), and few studies have been done on developing a universal retracker that is effective for all kinds of waveforms (Passaro, *et al.,* 2014).

The new generation of SARAL/AltiKa Ka-band satellite altimetry mission was launched into orbit in February 2013. The AltiKa mission carries a dual-frequency radiometer operating at 24 GHz and 37 GHz. The enhanced frequencies lead to a better vertical

ARPN Journal of Engineering and Applied Sciences

resolution and improving the spatial resolution, thanks to the Ka-band smaller footprint (8 km diameter compared to 20 km for Jason-2 and 15 km for ENVISAT, Verron, *et al.,* 2015). This contributes to decreasing no-data gap about 2-8 km to the coastline subject to the coastal characteristics (cf. Abdullah, *et al.,* 2016; Palanisamy, *et al.,* 2015).

AltiKa mission has been through a global calibration conducted by numerous agencies (e.g. The Centre National d'Etudes Spatiales (CNES), The Indian Space Research Organisation (ISRO) and European Space Agency (ESA)), and researchers (e.g. Abdalla, 2015, Palanisamy, *et al.,* 2015, Rémy, *et al.,* 2014, Valladeau, *et al.,* 2015, Dettmering, *et al.,* 2014). However, a limited number of studies have been conducted to validate the AltiKa retracked SLAs over marginal seas such as the South China Sea, Strait of Malacca and Sulu Sea. Regional validation is crucial since the ocean characteristics there are unique, consisting of many small islands and narrow straits, and lie above a wide continental shelf with an average water depth of 200 m. The region is situated in the tropics, where heavy rain and cloudy conditions are usually experienced. Since one of the major drawbacks of Ka-band is its sensitivity to the atmospheric liquid water (rain and cloud) which can lead to signal attenuation (Palanisamy, *et al.,* 2015), regional validation is crucial to access the data accuracy before it can be used in any applications.

In this paper, we examine the quality of SLAs derived from three retracking solutions: MLE-4, Ice-1 and Ice-2, provided in the Archiving, Validation, and Interpretation of Satellite Oceanographic (AVISO) Geophysical Data Product (GDR). Validation of retracked SLAs is performed in twofold: 1) comparison with quasi-independent geoid data and independent data from tide gauges. Comparison with geoid data provides information about the precision of the retracked SLAs, meanwhile comparison with tide gauges merits finding both the accuracy and precision of the SLA estimates.
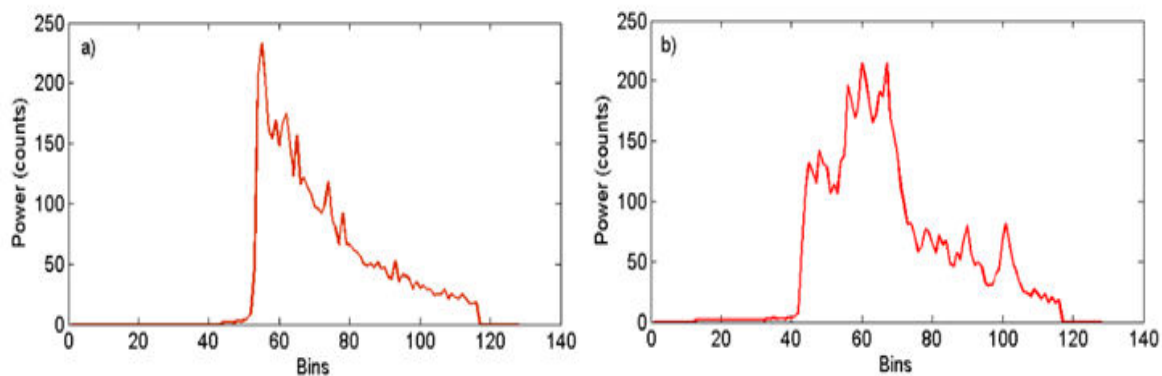

Figure-1. The example of return waveform. a) Brown-shape waveform over homogeneous ocean surface. b) Non-Brown waveform over complex coastal area.

2. DATA AND EXPERIMENTAL REGION

The experimental region is conducted over the South China Sea and its adjacent seas (as in Figure-2), which consists of the Andaman Sea, Strait of Malacca, Gulf of Thailand, South China Sea and Sulu Sea. These regions are selected due to their complex topographies. They consist of many small islands, peninsulas and shallow seas, which can produce complicated waveform patterns when they enter the altimeter footprint. They are also located in a tropical climate zone with various weather system causing diurnal rainfalls and cyclones that also contribute to diverse and complex altimetric waveform patterns (Strachan and Vidale, 2013).

The high (40 Hz) resolution along-track of AltiKa Geophysical Data Record (GDR) product version T are utilized in this study. The data are retrieved from AVISO ftp site (ftp://avisoftp.cnes.fr). The data are from cycles 1-19, which correspond to March 2013-December 2014.

For analysis and validation purposes, geoid height that is based on the Earth Gravitational Model 2008 (EGM2008) are used in the IMP computation to compute the precision of the retracked SLAs. The datasets are provided in the GDR product. To compute the accuracy of retracked SLAs, data from five tide gauge stations (Figure-2) are utilized. The hourly tide gauge data are obtained from Department of Survey and Mapping Malaysia (DSMM) and the University of Hawaii Sea Level Centre (UHSLC). Tide gauges at Lubang (13.82°N, 120.21°E), Bintulu (3.26°N, 113.06°E), Geting (6.23°N, 102.11°E), Ko Taphao Noi (7.82°N, 98.42°E) and Vung Tau (10.33°N, 107.07°E) stations are used to validate the SLAs along the satellite tracks (blue lines as in Figure-2) of 006, 808, 494, 537 and 479, respectively.
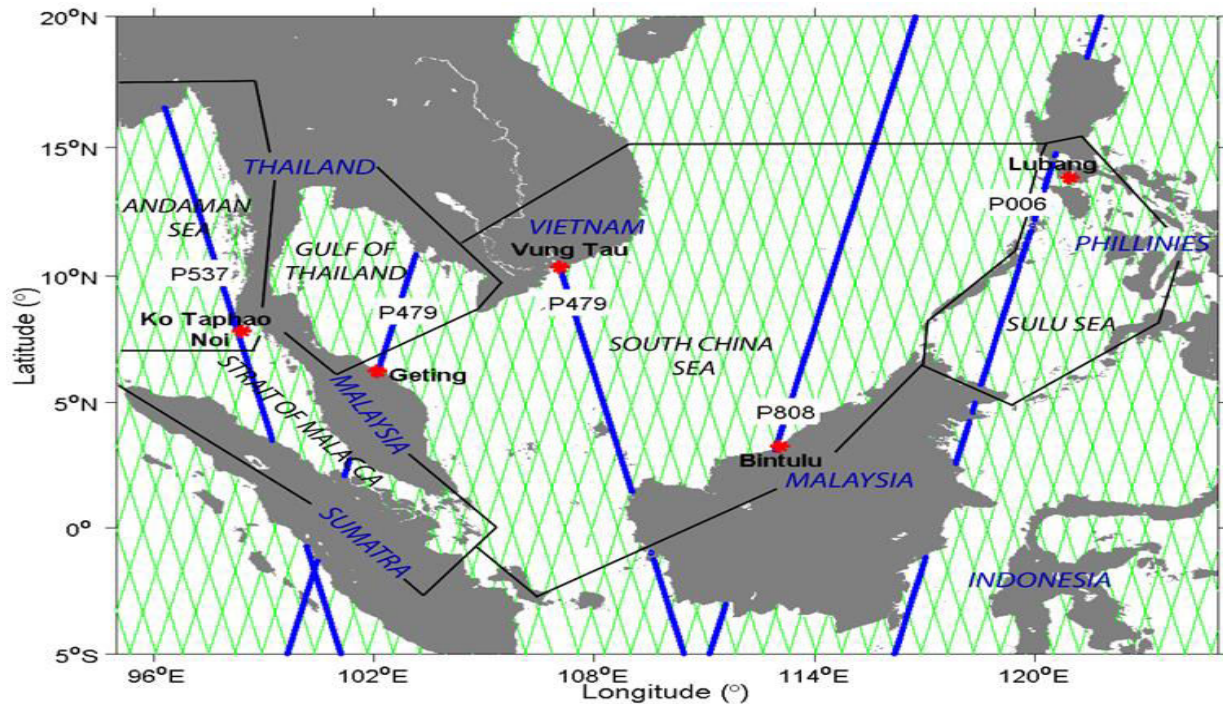
www.arpnjournals.com

Figure-2. The experimental region over the Andaman Sea, Gulf of Thailand, Strait of Malacca, South China Sea and Sulu Sea. Red marks show the tide gauge stations, and blue lines show the AltiKa tracks used for validation with tide gauges.

3. METHODOLOGY

Sea level anomaly (SLA) from AltiKa can be extracted as in equation 1 (Andersen and Scharroo, 2011);

$$SLA = H - (R_{obs} - R_{retracked} - \Delta R_{wet} - \Delta R_{dry} \qquad (1)$$

where H is satellite altitude, R_{obs} is observed range, $R_{retracked}$ is range correction from retracking algorithm, R_{dry} is dry tropospheric correction, R_{wet} is wet tropospheric correction, R_{iono} is ionospheric correction, R_{ssb} is sea state bias correction, $mssh$ is mean sea surface height and h_{ot} is ocean tides, h_{solid} is solid earth tides, h_{pole} is pole tides, h_{load} is tidal loading, h_{iny} is inverse barometer height correction, and h_{hf} is high frequency fluctuations. $R_{retracked}$ are the corrections from MLE-4, Ice-1 and Ice-2 retracking algorithms, R_{dry} and R_{wet} corrections are from the European Centre for Medium-Range Weather Forecasts, R_{iono} is from the Global Ionospheric Map, R_{ssb} is from the Hybrid sea state bias (Wang, *et al.,* 2010) and h_{ot} is from the FES2012 model.

The MLE-4 retracker is based on the Hyne (1980) model. It is a physical-based ocean model retracking method which is developed to fit the returned waveforms to the Brown (1977) model (cf. Deng and Featherstone, 2006, Lee, *et al.,* 2010). The MLE-4 retracker is an optimal way of fitting noisy altimeter waveform (Thibaut, *et al.,* 2010). It estimates the geophysical parameters of sea level, significant wave height, wind speed and off-nadir angle by determining the value that maximizes the probability of obtaining the recorded waveform shape in the presence of noise of a given statistical distribution (Gómez-Enri, *et al.,* 2007). The Ice-1 and Ice-2 retrackers are empirical-based

retrackers. The Ice-1 retracker uses the mean power of the waveform amplitude calculated using Offset Center of Gravity (OCOG) retracking algorithm (Lee, *et al.,* 2010, Wingham, *et al.,* 1986). The OCOG retracker was developed to find the centre of gravity of the waveform based on the power level within the waveform gates (Wingham, *et al.,* 1986). The Ice-1 retracker is well adapted to the rapidly changing surface. The Ice-2 retracker is a minor modification of the Brown (1977) model. It was developed for continental ice sheets. The leading edge of return waveform is modelled by Gaussian error function and the trailing edge modelled by exponential decaying function (Ganguly, *et al.,* 2015, Legresy, *et al.,* 2005).

For comparison with geoid height, the sea level above a referenced ellipsoid (SSH) is used. It was derived from Equation 1 without applying the subtraction from the mssh. For the validation with tide gauge, the retracked SLAs (above mssh) are validated with the SLAs from tide gauge observations. To be consistent, inverse barometric correction has not been applied to both altimeter and tide gauge SLAs. Tide gauge observations are filtered using a Loess Low Pass Filter (cf. Saraceno, *et al.,* 2008) with a 40-hour cut off wavelength to suppress the high frequency variations in the velocity data. The vertical motion of the land is not corrected from the tide gauge SLAs because it requires a Global Positioning System receiver to be attached at the tide gauge station, which is unavailable at tide gauges used in this study. The mean of SLA time series are removed from both altimeter and tide gauge to reduce biases in the vertical reference system between both datasets.

4. RESULTS AND DISCUSSION

The quality of retracked SLAs is assessed by computing the percentage of data availability near shore (Section 4.1). Comparison with geoid height is conducted to assess the data precision by computing the improvement of percentage (IMP) (Section 4.2), and comparison with tide gauge observation is performed to identify the accuracy and precision of retracked SLAs over the tested area (Section 4.3). They are determined based on the correlation coefficient and root mean square (RMS) error between both measurements.

For the computation of data availability and comparison with geoid height, the analysis is performed based on the along-track data within 30 km from the coastline. The tested regions include Andaman Sea, Sulu Sea, Gulf of Thailand, South China and Strait of Malacca (see Figure-2).

a) Data availability near shore

In this section, the mean percentage of SLA data availability within 30 km from the coastline for the five tested regions is computed for the retrackers of MLE-4, Ice-1 and Ice-2 (see Figure-3). For the purpose of quality control, outliers falling outside the three standard deviations are removed from the computation.

In general, all retrackers provide excellent data coverage with a high percentage of data availability (>80%) for all regions, except for Andaman Sea and Sulu Sea where data availability is 64-76%. Of all regions, the South China Sea has the highest (>88%) percentage with Ice-1, Ice-2 and MLE-4 retrackers provide 90%, 89% and 88% of data, respectively. The South China Sea has less complicated coastal topography when compared to the other regions. Therefore, the effect of land within the altimeter footprint may not be severe in this area, thus making the retracking of SLAs work efficiently and producing excellent data coverage.

In contrast, Sulu Sea has the lowest (<68%) percentage of data availability with Ice-1, Ice-2 and MLE-4 retrackers provide 68%, 65% and 64%, respectively. Sulu Sea is one of a complex of archipelagos, which consist of many small islands, narrow straits and shallow water with rough bottom topography. This region also suffers from quasi periodic-variation of surface roughness and rapid changes in sea-state (Apel, *et al.,* 1985). Due to the high complexity of the coastal topography, altimetric waveforms could be severely corrupted, thus producing erroneous estimates of geophysical information (Gommenginger, *et al.,* 2011).

Based on the results in Figure-3, four of five regions have data availability more than 70%, thanks to the smaller AltiKa footprint that has contributed to improving the segregating type of surface in transition zone (from water to land and from land to water) over coastal areas. It is also realized that the performance of Ice-1 retracker is always better than those of the Ice-2 and MLE4 retrackers, except at Andaman Sea where the performance of Ice-1 and Ice-2 are similar.

Previous research has confirmed that AltiKa altimetry provides significant improvement in accuracy and data availability up to ~3 km from the coastline (Abdullah, *et al.,* 2016), which is overwhelmingly better than Jason-2 and Envisat that can generally provide data beyond ~7-10 km to the coast (Babu, *et al.,* 2015, Deng and Featherstone, 2006, Idris and Deng, 2012).
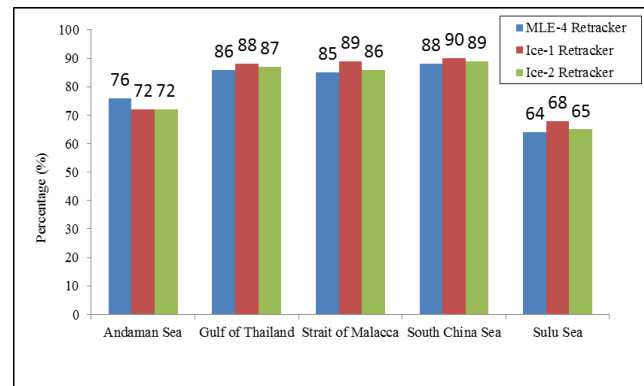

Figure-3. Percentage of SARAL/AltiKa retracked data availability over the experimental regions computed within 30 km from the coastline.

b) Validation of retracked sea level with geoid height

The precision of retracked SSHs with respect to geoid heights are assessed by computing the IMP within 30 km from the coastline. It is noted that the SSH and geoid height are referenced to different ellipsoids. The conversion of the reference ellipsoid is not performed because the impact on the analysis is assumed to be insignificant because the IMP is computed over short SSH profiles (~30 km from the coastline) or small areas. The IMP can be computed as equation 2 (Hwang, *et al.,* 2006):

$$IMP = \frac{\sigma_{MLE4} - \sigma_{retracked}}{\sigma_{MLE4}} \times 100 \qquad (2)$$

where σ_{MLE4} is the STD between MLE-4 retracked SSHs and geoid heights, and $\sigma_{retracked}$ is the STD between Ice-1 or Ice-2 retracked SSHs and geoid heights, respectively. In the computation of IMP, MLE-4 retracker is used as a reference because it is a standard retracker for the ocean. A positive value of IMP indicates that the precision of Ice-1 or Ice 2 retrackers is better than those of MLE-4 retracker.

Figure-4 shows the value of IMPs over the five experimental regions. It is seen that over Andaman Sea, Strait of Malacca and Sulu Sea, Ice-1 retracker has better precision with IMPs of 16%, 35% and 12%, respectively, than those of Ice-2 retracker, which has IMPs of 11%, 27% and 7%, respectively. However, different results are observed over the Gulf of Thailand and the South China Sea, where Ice-2 retracker has better precision with IMPs of 21% and 43%, respectively, meanwhile Ice-1 retracker has slightly lower IMP of 19% and 39%, respectively.

From Figure-4, it is realized that the value of IMPs for all regions are positive, which suggests that the

performance of Ice-1 and Ice-2 retrackers are always superior to those of the MLE-4 retrackers. This is an astonishing result as the Ice-1 retracker that is intended for hydrology and cryosphere applications, not for open ocean or coastal applications, outperforms the MLE-4 retracker.
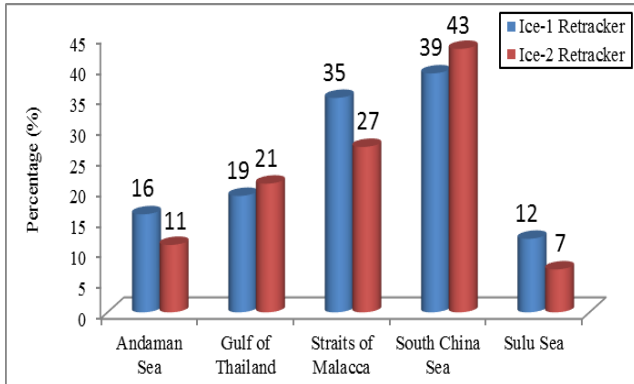

Figure-4. The IMP of Ice-1 and Ice-2 retrackers that are computed within 30 km from the coastline.

c) Validation of retracked sea level with tide gauges

The accuracy of retracked SLA is assessed by comparing with tide gauge observations. Five tide gauge stations (red mark in Figure-2) are used to validate the along-track AltiKa SLAs (blue line in Figure-2). The mean of temporal correlation and RMS error (Table-1) between both datasets is computed within 30 km from the coastline.

From Table-1, Ice-1 retracker shows superior results for pass 006 near Lubang (r= 0.81, RMS: 10 cm, see also Figure-5) and pass 537 near Ko Taphao Noi

(r=0.86, RMS: 6 cm, see also Figure-6), while Ice-2 retracker shows better results for pass 479 near Vung Tau (r= 0.82, RMS: 18 cm, see also Figure-7) and pass 494 near Geting (r=0.76, RMS: 34 cm, see also Figure-8). For pass 808 near Bintulu (see Figure-9), the correlation coefficients of MLE-4 and Ice-2 retrackers are similar (r=0.58), but the value of RMS error of MLE4 (12 cm) is slightly lower than those of the Ice-2 (15 cm).

Based on the results, Ice-1 retracker performs better than MLE-4 and Ice-2 retrackers over complex regions (i.e. Lubang and Ko Taphao Noi). These areas are surrounded with small islands and shallow water, which give significant impacts to the altimeter waveform signals. Land contamination within the altimeter footprint over these regions produces non-Brown like waveforms, which cannot be retracked by the retracking solutions (e.g. MLE-4 and Ice-2) that are based on the Brown (1977) model. Ice-1 retracker is an empirical-based retracker that does not rely on the physical shape of the waveform. It is based on Offset Centre of Gravity algorithm (Wingham, *et al.,* 1986), which is well adapted to the rapidly changes surface. Due to this, the Ice-1 retracker may be advantageous for those regions.

For less complicated areas with minimum land contamination such as Vung Tau and Geting, Ice-2 retracker shows better performance than MLE-4 and Ice-1 retrackers. Ice-2 retracker is a slight modification of the Brown (1977) model and can be used to optimize ocean-like waveforms for continental regions. Therefore, Ice-2 retracker may be advantageous for this region.

Table-1. Temporal correlation and rms error with respect to tide gauge stations computed within 30 km from the coastline.

Corresponding Ocean Region	Passes and Tide Gauge Stations		MLE-4	Ice-1	Ice-2
Sulu Sea	Pass 006 near Lubang	Correlation (r)	0.59	**0.81**	0.74
		RMS error (cm)	12	**10**	18
Andaman Sea	Pass 537 near Ko Taphao Noi	Correlation (r)	0.82	**0.86**	0.84
		RMS error (cm)	8	**6**	6
South China Sea	Pass 479 near Vung Tau	Correlation (r)	0.74	0.76	**0.82**
		RMS error (cm)	20	25	**18**
	Pass 494 near Geting	Correlation (r)	0.75	0.75	**0.76**
		RMS error (cm)	34	34	**34**
	Pass 808 near Bintulu	Correlation (r)	**0.58**	0.53	0.58
		RMS error (cm)	**12**	21	15

Examples of SLA time series for selective locations are shown in Figures 5-9. Results along pass 006 near Lubang (Figure-5) show that the retracked SLAs from all retrackers are limited to beyond 9 km from the coastline. Within 9 km of the coastline, many SLAs suffer

from data unavailability, making the interpretation of the result difficult over the area.

Along pass 537 near Ko Taphao Noi (Figure-6), high ($r \geq 0.80$) correlation of retracked SLAs is recorded as close as 1 km from the coastline suggesting good agreement between the retracked SLAs and the tide gauge.

www.arpnjournals.com

Along pass 479 near Vung Tau (Figure-7), no data are available within 6 km from the coastline. However, all retrackers perform well beyond 9 km from the coastline. That is the correlation ≥ 0.78. However, within 6 km from coastline, only Ice-2 retracker has high ($r=0.83$) correlation, meanwhile MLE-4 and Ice-1 retrackers have low correlation ($r\leq 0.52$). This suggest that the Ice-2 retracker explains more than 80% of the total variance, while MLE-4 and Ice-1 retrackers explain <50% of the total variance.

Along pass 494 near Getting (Figure-8), high ($r=0.71$) correlation is observed for Ice-1 retracker as close as 1 km from coastline. Meanwhile, along pass 808 near Bintulu (Figure-9), low ($r\leq 0.54$) correlation is observed from all retrackers within 1-3 km. Beyond 6 km from coastline, all retrackers are highly correlated ≥ 0.80 with tide gauge SLA, suggesting they have good agreement.
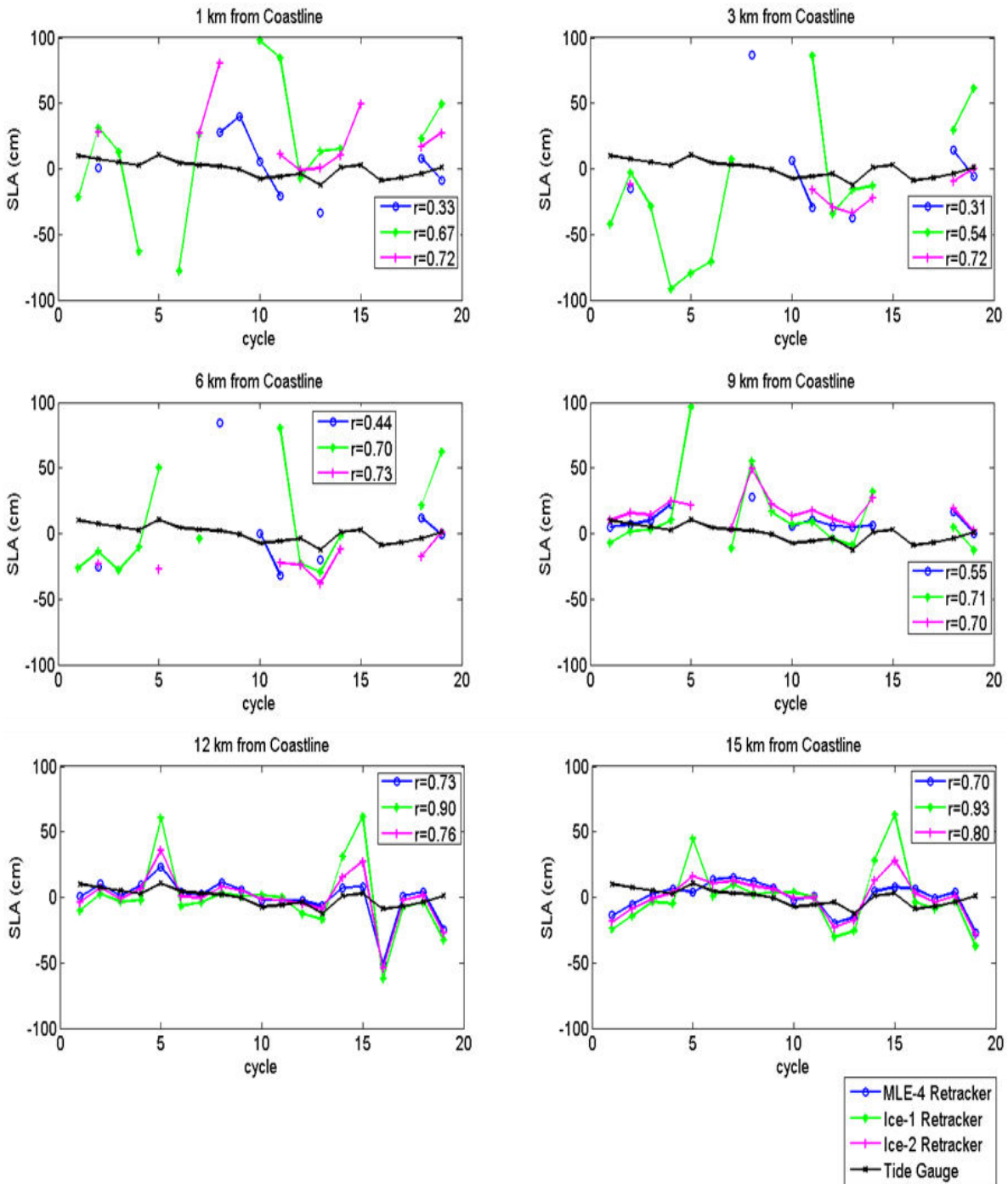

Figure-5. SLA time series along pass 006 near Lubang tide gauge station.
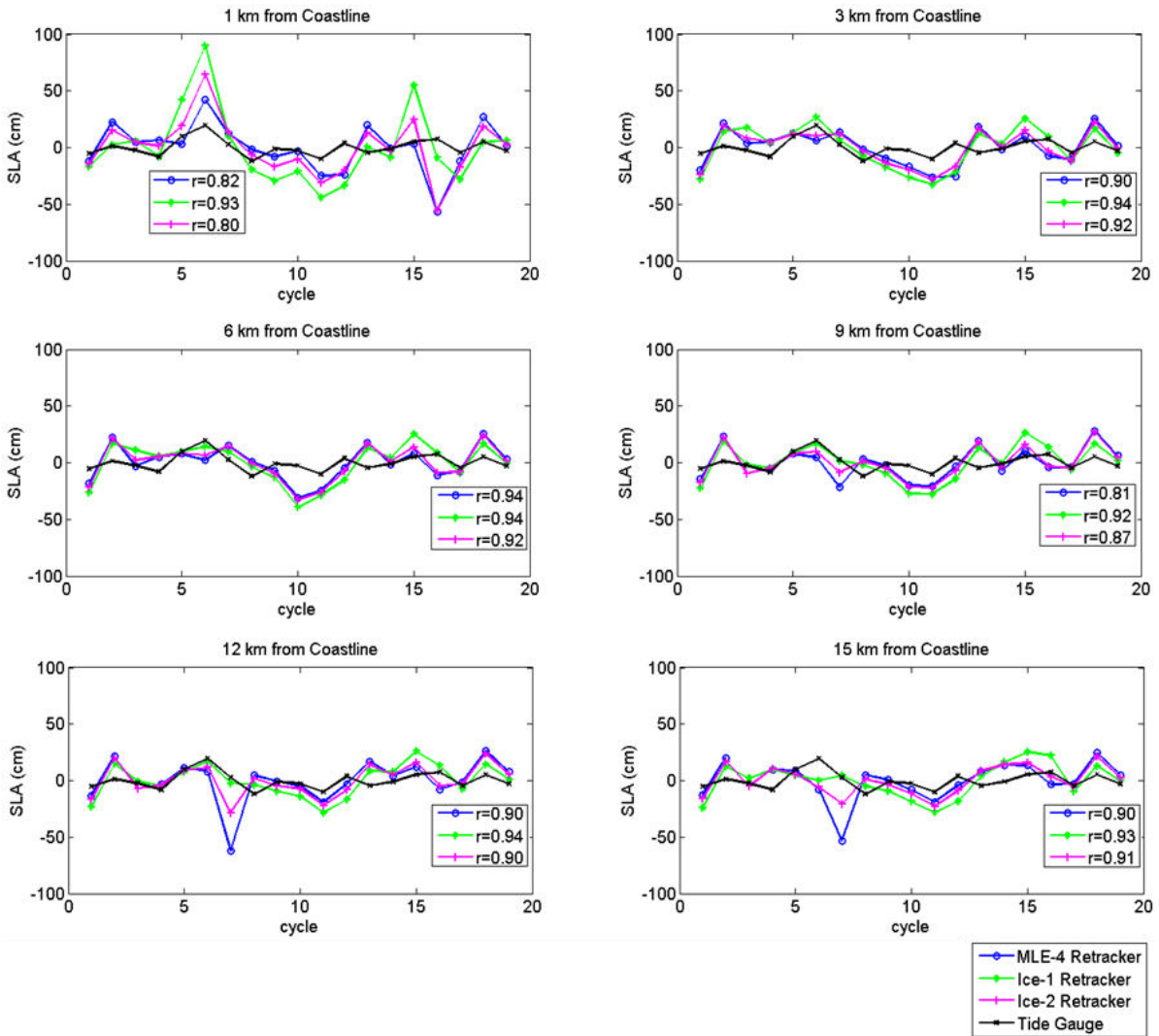
www.arpnjournals.com

Figure-6. SLA time series along pass 537 near Ko Taphao Noi tide gauge station.

Figure-7. SLA time series along pass 479 near Vung Tau tide gauge station.
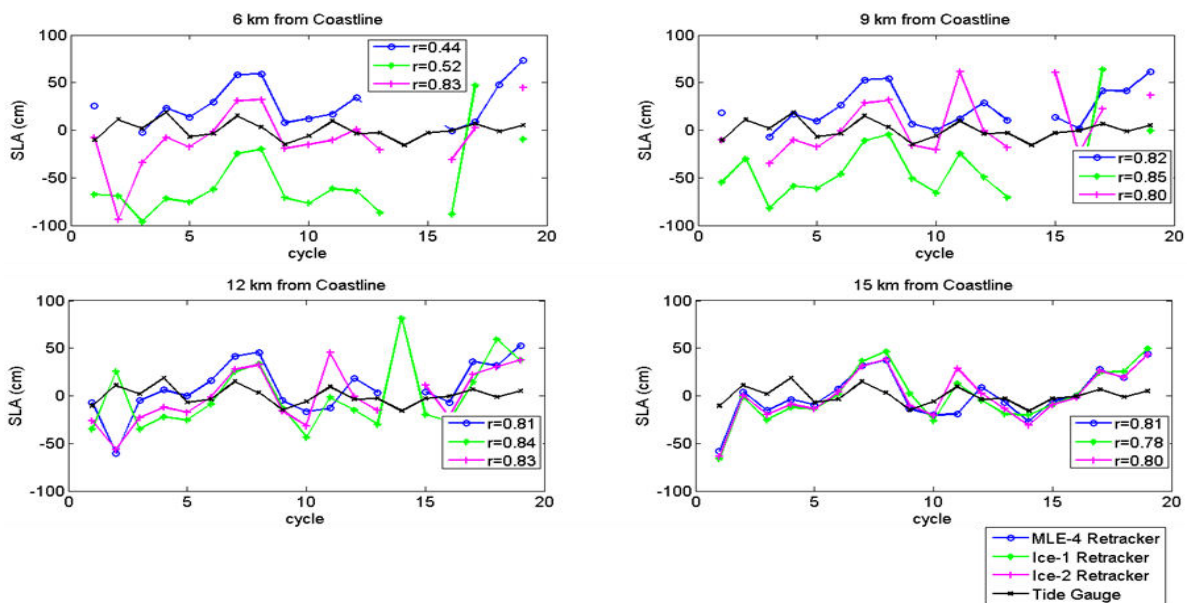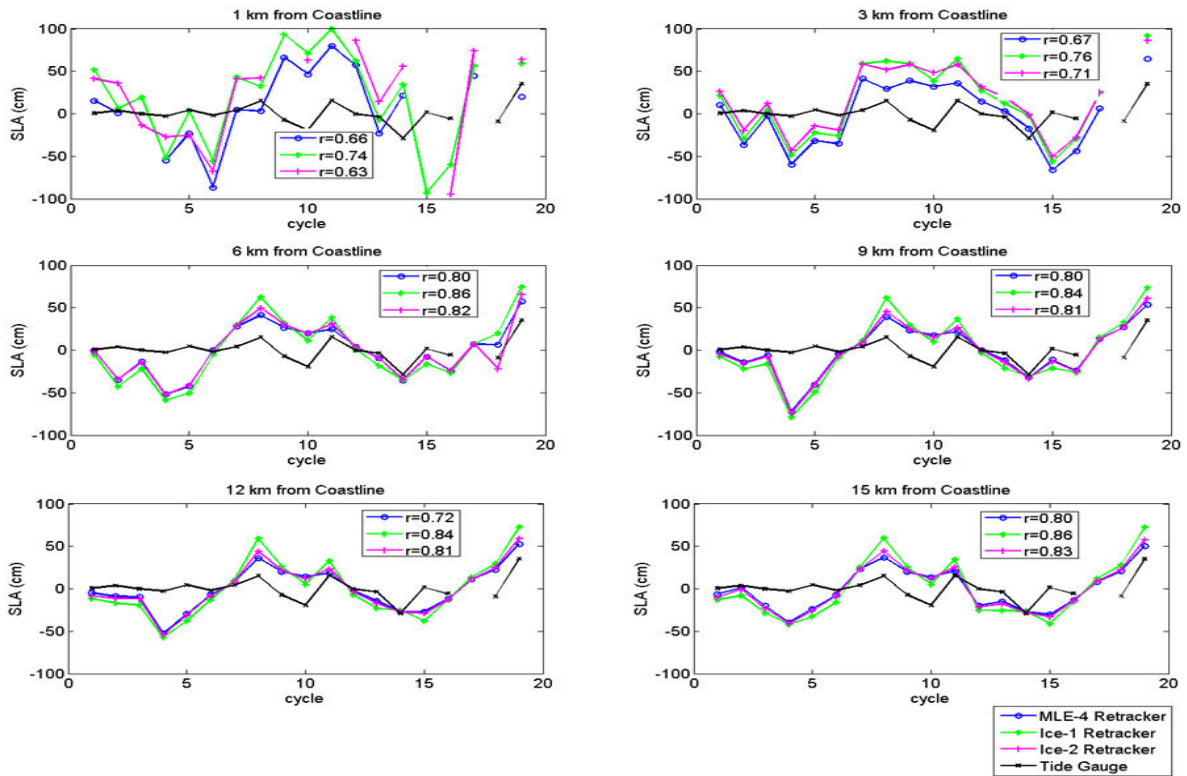
www.arpnjournals.com

Figure-8. SLA time series along pass 494 near Geting tide gauge station.

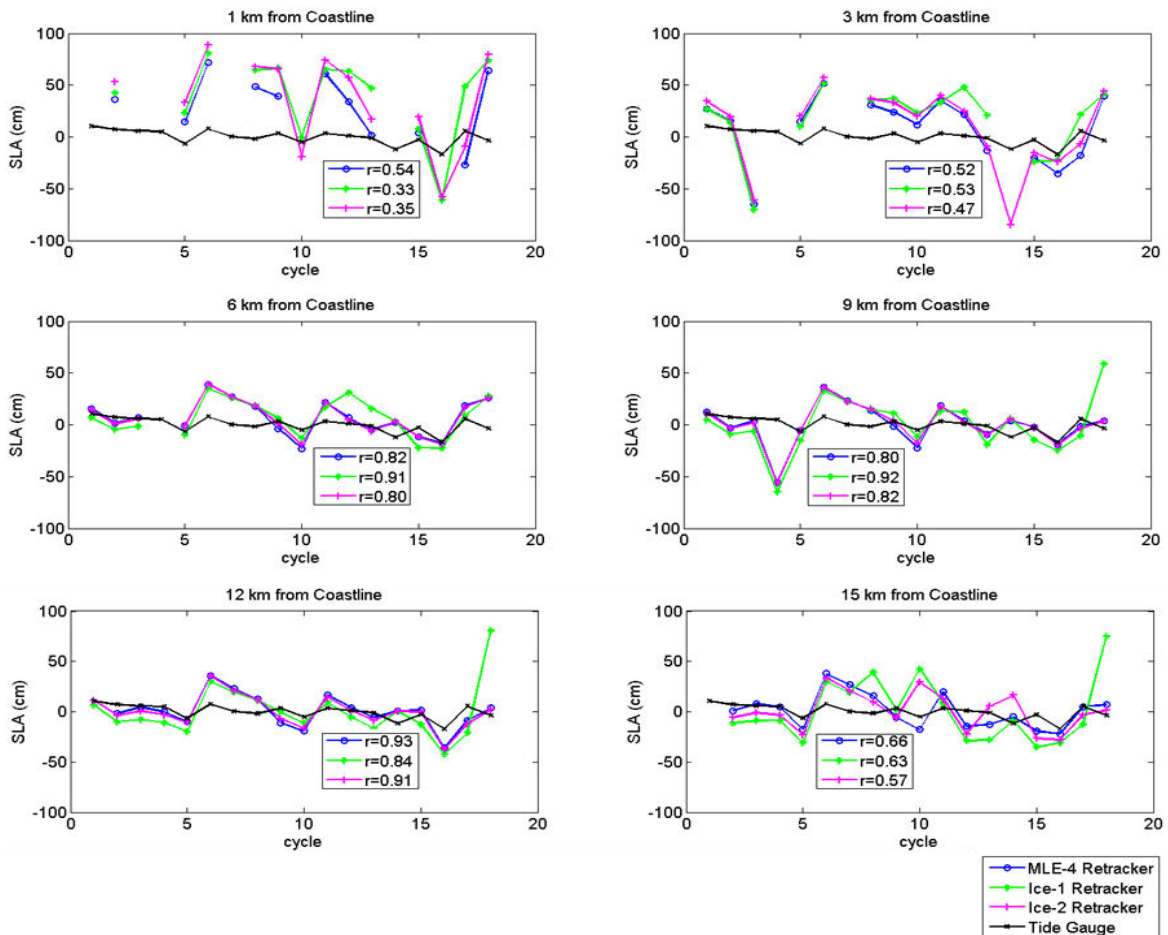**Figure-9.** SLA time series along pass 808 near Bintulu tide gauge station.

www.arpnjournals.com

5. CONCLUTION

The results obtained from the validation with tide gauges are consistent with the findings from the validation against geoid height. It can be summarized that for the South China Sea region, Ice-2 retracker is the optimum retracking solution since it provides excellent data coverage (89%) and high IMP (43%). Two out of three tide gauge stations that are situated over the South China Sea record the highest temporal correlation and the lowest RMS error of Ice-2 retracked SLAs. That is, 0.82 and 18 cm, respectively for Vung Tau, and 0.76 and 34 cm, respectively for Getting. However, for Bintulu, the correlation of Ice-2 and MLE-4 retrackers is similar (0.58), but MLE-4 has slightly lower (12 cm) RMS error compared to Ice-2 (15 cm) suggesting that MLE-4 retracker has better accuracy than those of Ice-2.

For Sulu and Andaman Sea, Ice-1 retracker is optimum because it provides excellent data coverage of 68% and 72%, respectively, and high IMP (12% and 16%, respectively). For Sulu Sea, Lubang tide gauge station records the highest correlation of 0.81 and the lowest RMS error of 10 cm when compared to the other two retrackers. For Andaman Sea, Ko Taphao Noi tide gauge station records the highest correlation of 0.86, and the lowest RMS error of 6 cm. It is noted that the discussion does not include the Gulf of Thailand because the tide gauge data are unavailable for the year 2013 to2014.

It is noted that tide gauge data were not commonly used to validate the altimeter over the South China Sea region. This is because the possible effect of tidal correction error on the altimeter derived sea level to the short time series of altimeter was not sufficiently discussed (Han and Huang, 2009). However, lacking of other in-situ data over the region is one of the major challenge in validation purposes. There is no high frequency (HF) radar available over this region.

Further research is currently undertaken to include longer time series datasets in the analysis. This is important as to analysis and removing the tidal signals from the SLAs. Nonetheless, the already prevailing high correlations and low RMS errors between SARAL/AltiKa sea level and tide gauges assure that the quality of the sea level data may be defined as superior for the experimental coastal regions.

ACKNOWLEDGEMENTS

REFERENCES

[1] Abdalla S., 2015, SARAL/AltiKa Wind and Wave Products: Monitoring, Validation and Assimilation. Marine Geodesy, 38 (sup1), 365-80, doi:10.1080/01490419.2014.1001049.

[2] Abdullah N., Idris, N. and Maharaj A., 2016, The Retracked Sea Levels from SARAL/AltiKa Satellite Altimetry: the Case Study around the Strait of Malacca and the South China Sea. International Journal of Geoinformatics, 12 (2), 33-39.

[3] Andersen O. B. and Scharroo R., 2011, Range and Geophysical Corrections in Coastal Regions: And Impications for Mean Surface Determination. Chap. 5 In Coastal Altimetry, edited by Vignudelli, S., Kostianoy, A. G., Cipollini, P. and Benveniste, J., 103-46. (London, New York: Springer).

[4] Apel J. R., Holbrook J. R., Liu A. K. and Tsai J. J., 1985, The Sulu Sea Internal Soliton Experiment. Journal of Physical Oceanography, 15 (12), 1625-51.

[5] AVISO. 2010, Coastal and Hydrology Altimetry Product Handbook. in. http://www.aviso.oceanobs.com/fileadmin/documents /data/tools/hdbk_Pistach.pdf

[6] Babu K., Shukla A., Suchandra A., Arun Kumar S., Bonnefond P., Testut L., Mehra P. and Laurain O., 2015, Absolute Calibration of SARAL/Altika in Kavaratti During its Initial Calibration-Validation Phase. Marine Geodesy, 38 (sup1), 156-70.

[7] Bao L., Lu Y. and Wang Y., 2009, Improved Retracking Algorithm for Oceanic Altimeter Waveforms. Progress in Natural Science, 19 (2), 195-203, doi:10.1016/j.pnsc.2008.06.017.

[8] Berry P. A. M., Sanders R. F., Leemans C. and Bron E., 1998, Generating Orthometric Heights from The Ers-1 Altimeter Geodetic Mission Dataset: Results from an Expert System Approach. In Geodesy on the move. International Association of Geodesy Symposia, edited by Forsberg, R., Feissl, M. and Deitrich, R., (Verlag, Berlin, Germany: Springer).

[9] Brown G. S., 1977, The Average Impulse Response of a Rough Surface and its Applications. IEEE J. Oceanic Eng., 2, 67 – 74.

[10] Deng X. and Featherstone W. E., 2006, A Coastal Retracking System for Satellite Radar Altimeter Waveforms: Application to ERS-2 around Australia. Journal of Geophysical Research, 111 (C6), 12-28, doi:10.1029/2005jc003039.

[11] Deng X., Featherstone W. E., Hwang C. and Berry P. A. M., 2002, Estimation of Contamination of ERS-2

and POSEIDON Satellite Radar Altimetry Close to the Coasts of Australia. Marine Geodesy, 25 (4), 249-71, doi:10.1080/01490410214990.

[12] Fernandes J., Nunes A. L., Lazaro C., Pires N., Bastos L. and Mendes V. B., 2008, Wet Trophospheric Correction for Coastal Altimetry Based on GNSS Path Delay Measurement. Paper presented at the Coastal Altimetry Workshop, 6-7 November, in Pisa, Italy.
http://www.coastalt.eu/files/pisaworkshop08/pres/03-Fernandes_etal_2ndWCA_vf2.pdf

[13] Ganguly D., Chander S., Desai S. and Chauhan P., 2015, A Subwaveform-Based Retracker for Multipeak Waveforms: A Case Study over Ukai Dam/Reservoir. Marine Geodesy, 38 (sup1), 581-96.

[14] Gómez-Enri J., Gommenginger C. P., Srokosz M. A., Challenor P. G. and Benveniste J., 2007, Measuring Global Ocean Wave Skewness by Retracking RA-2 Envisat Waveforms. Journal of Atmospheric and Oceanic Technology, 24 (6), 1102-16, doi:10.1175/jtech2014.1.

[15] Gommenginger C., Thibaut P., Fenodlio-Marc L., Quartly G., Deng X., Gomez-Enri J., Challenor P. and Gao, Y., 2011, Retracking Altimeter Waveforms Near the Coasts. A Review of Retracking Methods and Some Applications to Coastal Waveforms. Chap. 4 In Coastal Altimetry, edited by Vignudelli, S., Kostianoy, A. G., P.Cipollini and Benveniste, J., 61-101. (London, New York: Springer).

[16] Han G. and Huang W., 2009, Low-frequency sea-level variability in the South China Sea and its relationship to ENSO. Theoretical and applied climatology, 97 (1-2), 41-52.

[17] Hwang C., Guo J., Deng X., Hsu H. Y. and Liu Y., 2006, Gravity Anomalies in Coastal Waters from Retracked Geosat/GM Altimetry: Comparison with Ship Borne and Airborne Gravity Data. Journal of Geodesy, 80 (4), 204 -16, doi:10.1007/s00190-006-0052-x.

[18] Hyne G. S., 1980, Radar Altimeter Mean Return Waveforms from Near-normal-incidence Ocean Surface Scattering. IEEE Transaction on Antennas and Propagation, 25 (5), 687 – 92.

[19] Idris N. H. and Deng X., 2013, An Iterative Coastal Altimetry Retracking Strategy Based on Fuzzy Expert System for Improving Sea Surface Height Estimates. Proceedings of Geosciences and Remote Sensing Symposium (IGARSS), 2954-57, IEEE International, doi:10.1109/IGARSS.2013.6723445.

[20] Idris N. H. and Deng X., 2012, The Retracking Technique on Multi-Peak and Quasi-Specular Waveforms for Jason-1 and Jason-2 Missions near the Coast. Marine Geodesy, 35, 217-37, doi:10.1080/01490419.2012.718679.

[21] Kuo H. T., Shum C. K., Chao Y., Emery W. J., Fok H., Lee H., Kuo C.-Y. and Yi Y., 2011, Radar Altimetry Waveform Retracking Applied to Coastal Ocean. Paper presented at the 5th Coastal Altimetry Workshop, 16-18 October, in San Diego, USA.
http://www.coastalt.eu/files/sandiegoworkshop11/poster/P33_Tseg_OSTST_CoastalWater11.pdf

[22] Lee H., Shum C. K., Emery W., Calmant S., Deng X., Kuo C.-Y., Roesler C. and Yi Y., 2010, Validation of Jason-2 Altimeter Data by Waveform Retracking over California Coastal Ocean. Marine Geodesy, 33 (sup1), 304-16, doi:10.1080/01490419.2010.488982.

[23] Lee H., Shum C. K., Yi Y., Braun A. and Kuo C.-Y., 2008, Laurentia Crustal Motion Observed using Topex/Poseidon Radar Altimetry over Land. Journal of Geodynamics, 46 (3-5), 182-93, doi:10.1016/j.jog.2008.05.001.

[24] Legresy B., Papa F., Remy F., Vinay G., Van Den Bosch M. and Zanife O.-Z., 2005, ENVISAT Radar Altimeter Measurements over Continental Surfaces and Ice Caps using The Ice-2 Retracking Algorithm. Remote Sensing of Environment, 95 (2), 150-63.

[25] Obligis E., Desportes C., Eymard L., Fernandes J., Lazaro C. and Nunes A. L., 2011, Tropospheric Corrections for Coastal Altimetry Chap. 6 In Coastal Altimetry, edited by Valladeau, G., Kostianoy, A. G., Cipollini, P. and Benveniste, J., 147 - 76. (Berlin: Springer).

[26] Obligis E., Mercier F., Picard B. and Desportes C., 2008, Land Decontamination Method for Wet Trophospheric Correction Retrieval. Paper presented at the Coastal Altimetry Workshop, 6 -7 November, in Pisa, Italy.

[27] Palanisamy H., Cazenave A., Henry O., Prandi P. and Meyssignac B., 2015, Sea-Level Variations Measured by the New Altimetry Mission SARAL/AltiKa and its Validation Based on Spatial Patterns and Temporal Curves Using Jason-2, Tide Gauge Data and an Overview of the Annual Sea Level Budget. Marine Geodesy, 38 (sup1), 339-53, doi:10.1080/01490419.2014.1000469.

[28] Passaro M., Cipollini S., Vignudelli G. Q. and Snaith H. M., 2014, ALES: A Multi-mission Adaptive Subwaveform Retracker for Coastal and Open Ocean Altimetry. Remote Sensing Environment, 145, 173-89, doi:10.1016/j.rse.2014.02.008.

www.arpnjournals.com

[29] Quartly G., 2010, Hyperbolic Retracker: Removing Bright Target Artifacts from Altimetric Waveform Data, Paper presented at the In Proceeding of ESA Living Planet Symposium, June, in Bergen. ESA SP-686.

[30] Rémy F., Flament T., Michel A. and Blumstein D., 2014, Envisat and SARAL/AltiKa Observations of the Antarctic Ice Sheet: A Comparison Between the Ku-band and Ka-band. Marine Geodesy, 38 (sup1), 510-21, doi:10.1080/01490419.2014.985347.

[31] Saraceno M., Strub P. T. and Kosro P. M., 2008, Estimates Of Sea Surface Height and Near-Surface Alongshore Coastal Currents from Combinations of Altimeters and Tide Gauges. Journal of Geophysical Research, 113 (C11), 20pp, doi:10.1029/2008jc004756.

[32] Strachan J. and Vidale P. L., 2013, Investigating Global Tropical Cyclone Activity with a Hierarchy of AGCMs: The Role of Model Resolution. Journal of Climate, 26 (1), 133-52, doi:http://dx.doi.org/10.1175/JCLI-D-12-00012.1.

[33] Thibaut P., Poisson J. C., Bronner E. and Picot N., 2010, Relative Performance of the MLE3 and MLE4 Retracking Algorithms on Jason-2 Altimeter Waveforms. Marine Geodesy, 33 (S1), 317 - 35, doi:10.1080/01490419.2010.491033.

[34] Thibaut P., Poisson J. C., Halimi A., Mailhes C., Tourneret J. Y., Boy F. and Picot N., 2011, A Review of CLS Retracking Solutions for Coastal Altimeter Workshop. Paper presented at the 5th Coastal Altimetry Workshop, 16-18 October, in San Diego, USA. http://www.coastalt.eu/files/sandiegoworkshop11/pres/12_Thibaut_CLS_Retracking_Review.pdf

[35] Thibaut P., Poisson J. C., Ollivier A., Bronner E. and Picot, N., 2009, Singular Value Decomposition

Applied on Altimeter Waveforms. Paper Paper presented at the OSTST meeting, 22-24 June, in Seattle, USA. http://www.aviso.oceanobs.com/fileadmin/documents/OSTST/2009/oral/Thibaut_SVD2.pdf

[36] Tseng K.-H., Shum C., Yi Y., Emery W. J., Kuo C.-Y., Lee H. and Wang H., 2014, The Improved Retrieval of Coastal Sea Surface Heights by Retracking Modified Radar Altimetry Waveforms. IEEE Transactions on Geoscience and Remote Sensing, 52 (2), 991-1001.

[37] Valladeau G., Thibaut P., Picard B., Poisson J. C., Tran N., Picot N. and Guillot A., 2015, Using SARAL/AltiKa to Improve Ka-band Altimeter Measurements for Coastal Zones, Hydrology and Ice. The PEACHI Prototype. Marine Geodesy, 38 (sup1), 124-42, doi:10.1080/01490419.2015.1020176.

[38] Verron J., Sengenes P., Lambin J., Noubel J., Steunou N., Guillot A., Picot N., Coutin-Faye S., Sharma R., Gairola R. M., Murthy D. V. A. R., Richman J. G., Griffin D., Pascual A., Rémy F. and Gupta P. K., 2015, The SARAL/AltiKa Altimetry Satellite Mission. Marine Geodesy, 38 (sup1), 2-21, doi:10.1080/01490419.2014.1000471.

[39] Wang D.-P., Flagg C. N., Donohue K. and Rossby H. T., 2010, Wavenumber Spectrum in the Gulf Stream from Shipboard ADCP Observations and Comparison with Altimetry Measurements. Journal of Physical Oceanography, 40 (4), 840-44, doi:10.1175/2009jpo4330.1.

[40] Wingham D. J., Rapley C. G. and Griffiths H., 1986, New Techniques in Satellite Tracking Systems. In IGARSS. Paper presented at the 86 Symposium Digest September, in Zurich, Switzerland.